*Paper Presented at the SMMA 2001 Fall Technical Conference "Emerging Technologies for Electric Motion Industry", Durham, North Carolina, USA, 3-5 Oct, 2001*

# Recent Advancement in the Thermal Design of Electric Motors

David Staton, Motor Design Ltd, dave.staton@motor-design.com
Stephen Pickering, University of Nottingham, Stephen.Pickering@nottingham.ac.uk
Desmond Lampard, University of Nottingham, des.lampard@nottingham.ac.uk

## Introduction

Traditionally electric motor manufactures have tended to concentrate effort on improving the electromagnetic design and have only dealt with the thermal design aspects superficially. However the increasing requirement for miniaturisation, energy efficiency and cost reduction, and the need to fully exploit new topologies and materials, make it imperative to analyse the thermal circuit to the same extent as the electromagnetic design.

This paper examines the thermal aspects that a design engineer should consider and how this fits into the overall design process. The improvements that can be achieved by properly accounting for the thermal circuit at the design stage will be demonstrated using two commercially available thermal CAE packages. One of the packages is based on the lumped-circuit technique, the other on computational fluid dynamics (CFD). The individual benefits of the two packages will be highlighted.

## Traditional Thermal Design Techniques

Traditionally the thermal performance of a new motor design has been estimated from prior knowledge of one or more of the following parameters - winding to ambient thermal resistance, housing heat transfer coefficient, winding current density limit or winding specific electric loading limit. These numbers may be estimated from tests on existing motors, from competitor catalogue data, or from simple rules of thumb [1-3]. The problem with such design methods is that no insight is gained of where the thermal design may be compromised and therefore where design effort should be concentrated. This is an area in which thermal lumped circuit analysis and CFD techniques can be used to successfully aid the design process.

## The Motor Design Process

The flow diagram of the ideal design process used to design and electric motor is shown in Fig 1. Starting with the design aims, ideally several possible solutions will be identified. During the implementation stage the best available design tools are used firstly to gain a thorough understanding of the problem and secondly to optimise the design. Typically, several software tools will be used at this stage, ranging from simple spreadsheet programs to sophisticated analytical and numerical computer aided engineering (CAE) packages. CAE tools should be used to study the electromagnetic, mechanical and thermal design aspects. The three areas of design are interrelated and iteration between the individual disciplines is required to obtain optimum design. For instance, in order to calculate the thermal rating of an electric motor, an iterative process between the motor losses and temperature distribution throughout the motor is required.

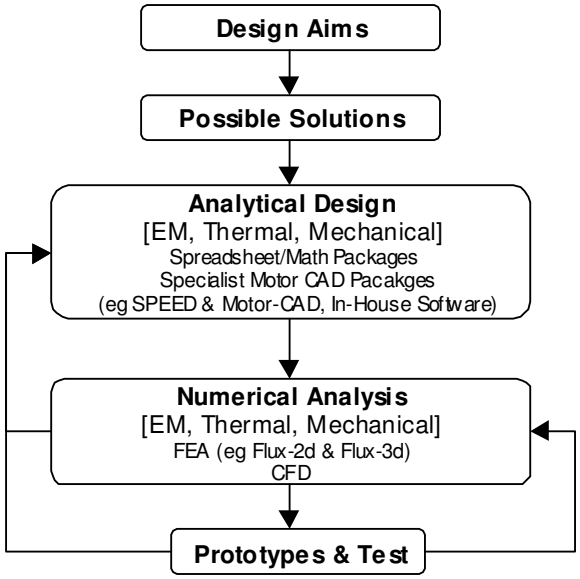


Fig 1: Flow diagram of ideal motor design process

The analytical design section of the flow diagram includes dedicated design packages for the electromagnetic and thermal design of motors. Often a design department will have their own proprietary software packages for the electromagnetic design of the motor types they are interested in. Alternatively, they may have a commercial software package such as the Speed software [4]. The thermal lumped circuit approach is the thermal design equivalent of specialist electromagnetic design packages used to size the magnetic circuit of the motor. A limitation of dedicated design packages is that they can only be used to design motor types that have been in-built into the software. However, such packages often have so many options and "adjustment factors" built in, that this situation occurs infrequently.

CFD is the thermal equivalent of electromagnetic FEA and is used to fine tune the design and analyse features that are beyond the simple calculation techniques.

This ideal design process is seldom followed as motor design departments often have deficiencies in their thermal design capabilities. In many cases only the thermal design is only examined rudimentary and in some cases overlooked completely. These deficiencies are especially common in companies involved in the design of smaller and medium sized machines, where prototypes are often built to try and overcome the shortcomings of the design process.

## Thermal Lumped Circuit Analysis

A commercially available lumped circuit analysis package, Motor-CAD [5], will be used to highlight some of the advantages that can be gained by carrying out thermal design in parallel with the electromagnetic design. In particular the package will be used to examine a selection of the thermal issues that may be considered when designing a new brushless permanent magnet motor. It will also be used to highlight some of the improvements that can be achieved by adopting some of the new manufacturing techniques and materials available. Data is presented to illustrate improvements achieved in particular designs. These values cannot however be generalised to all motors as each design is different and a complete thermal evaluation should be performed on all new designs.

The lumped circuit approach has a clear advantage over numerical techniques such as finite-element analysis (FEA) and computational fluid dynamics (CFD) techniques in terms of calculation speed. The near instantaneous calculation capabilities of the analysis technique make it possible to run "what-if" scenarios in real time. The main strengths of the numerical techniques are in the development of convection formulations for use in lump-circuit analysis [5-7], rather than carrying out the thermal circuit optimisation itself.

### Lumped Circuit Schematic

Figs 2 & 3 show typical schematic diagrams of a brushless permanent magnet motor lumped circuit model. A schematic diagram is useful for analysing steady-state thermal data. It is used to analyse thermal resistance, power flow and temperature distribution within the motor. In this particular package all the components are colour coded to match those shown in the cross-section editors (Fig's 4 & 5). In summary, the circuit consists of thermal resistances and heat sources connected between motor component nodes. Thermal resistance values for all conduction paths within the motor are calculated from motor dimensions and material data.

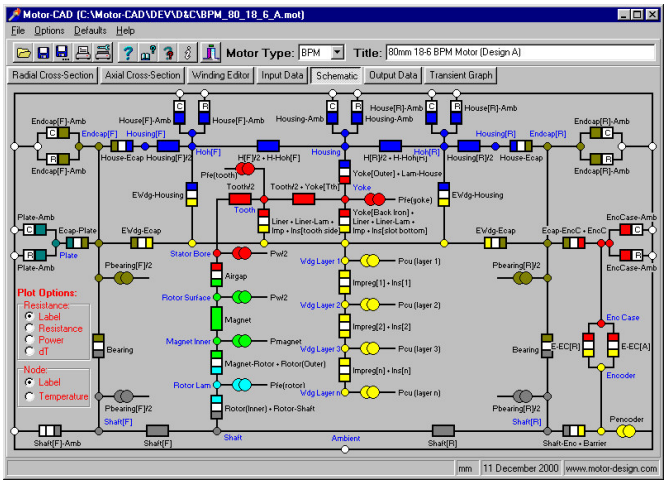


Fig. 2: Lumped circuit BPM thermal model

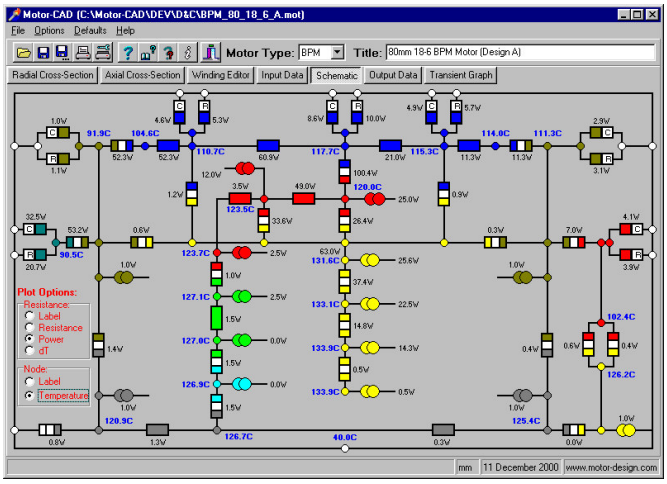


Fig. 3: Schematic showing motor power flow

### Contact Resistance

The accuracy of the calculation is dependent upon knowledge of the various thermal contact resistances between components within the motor, e.g. housing to lamination interface, slot-liner to lamination interface. Such resistances occur due to contact between solid surfaces taking place at limited numbers of high spots, the adjacent voids usually being filled with air. There has been much experimental work on the prediction of contact resistance [8,9]. Lumped circuit analysis combined with motor test data also forms an effective parameter identification tool. This technique can be used to estimate the gaps within the machine which are physically impossible to measure and to quantify the effects of winding impregnated air pockets.

## Cross-Section Editors

Radial & axial cross-section editors are used for dimensional data input (Figs 4 to 6). Figs 4 & 5 show a 80mm diameter concentrated winding motor design, in this case having 12 slots and 8 poles. Fig 6 shows a traditionally wound motor having 18 slots and 6 poles. It has the same diameter and axial length as the concentrated wound motor, however, its overall length is 30% longer to accommodate the longer end-turns.

The visual feedback produced helps the user gain an insight about the importance of the various heat paths within the motor. Thermal resistance is proportional to length and inversely proportional to cross-sectional area and thermal conductivity. The feedback also reduces the incidence of input errors.

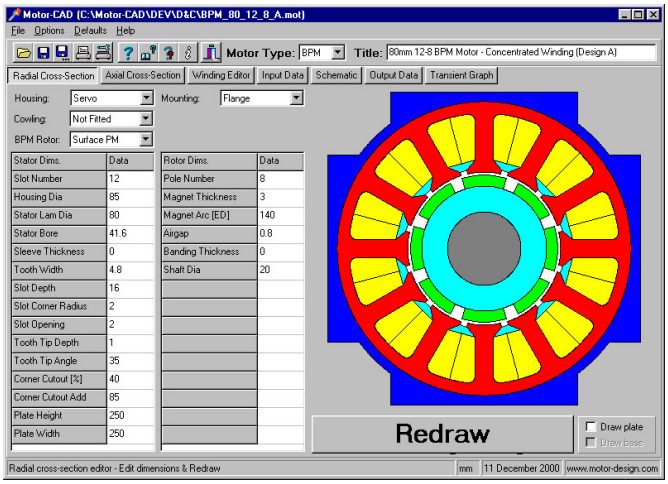


Fig. 4: Motor radial cross-section editor showing a 80mm diameter concentrated winding motor design

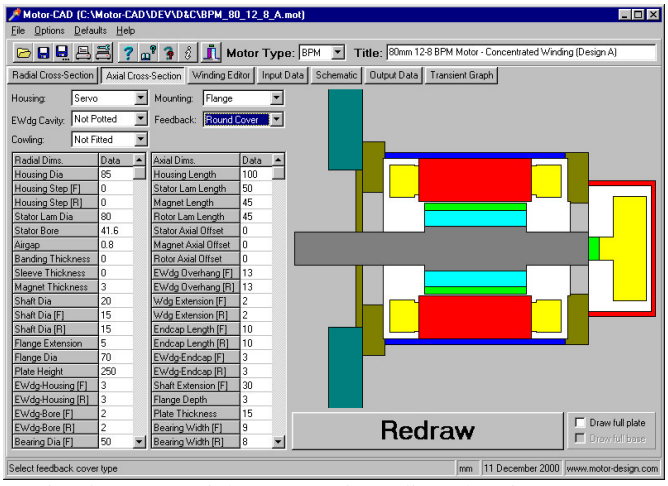


Fig. 5: Motor axial cross-section editor showing a 80mm diameter concentrated winding motor design

## Winding Design

The winding is modelled using several layers of copper, wire insulation and inter-conductor insulation (impregnation and/or air) together with a slot-liner and a slot-liner-lamination interface gap (Figs 7 & 8). The number of layers and copper to insulation thickness ratio is set by wire diameter, number of turns and subsequent slot-fill. The winding diagrams are useful for gaining a visual indication of the slot-fill that can be achieved using various winding techniques. For instance the winding shown in Fig 7 is for a traditional winding in which the coils are inserted into the slots through the slot openings. This is the winding used in the motor shown in Fig 6. Fig 8 shows the increased slot fill that can be achieved using a more modern concentrated winding in which the non-overlapping coils are precision wound directly onto a segmented tooth, the teeth then being joined together to form a wound stator. This is the winding used in the motor shown in Figs 4 & 5.

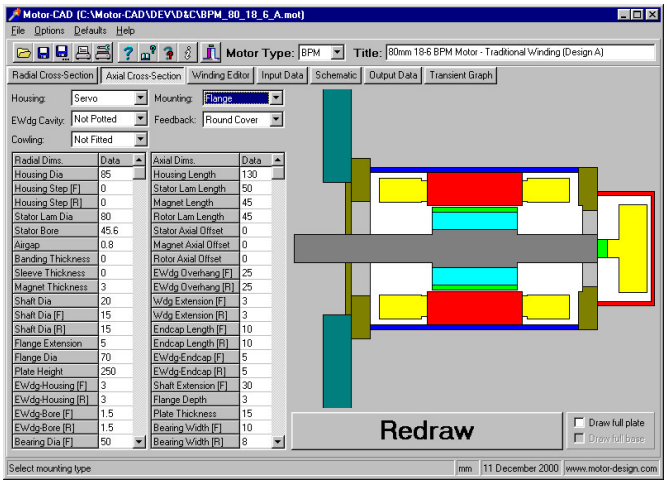


Fig. 6: Motor axial cross-section editor showing a 80mm diameter traditionally wound motor design

## Concentrated winding techniques

Fig 7 shows a traditional winding in which the coils are inserted into the slots through the slot openings. This has a slot-fill limit of around 55% (based on round covered conductors and slot area available for winding after liner insertion). Fig 8 shows the increased slot fill that can be achieved using a more modern concentrated winding in which the non-overlapping coils are precision wound directly onto a segmented tooth and the teeth are subsequently joined together to form a wound stator. Slot fills of around 80% can be achieved using this technique.

The windings shown in Figs 7 & 8 are used in the motors shown in Fig 6 & 5 respectively. It is seen that the non-overlapping winding benefits from having a shorter end-winding length. This also gives a reduction in resistance and

copper loss. For example, in the case of the 80mm diameter motor reported here, the 12-slot 8-pole concentrated winding design has a 100mm overall length compared to 130mm for the 18-slot 6-pole traditionally wound motor. It also produces 34% more torque for the same temperature rise.

A similar design study as that performed on the two 80mm diameter motors described above has been carried using two 160mm diameter motors. One was a 36-slot, 6-pole traditionally wound motor and the other a 12-slot, 8-pole concentrated wound motor, both having the same active length. In this case the 12-slot design has a overall length of 190mm compared to 230mm, but the torque increase for a given temperature rise is only 8%. The reduced improvement is largely due to the fact that the 36-slot motor has 80% more total slot periphery than the 12-slot motor to dissipate its copper. In the case of the 80mm motors, the 18-slot motor has only a 16% benefit in terms of total slot periphery compared to the 12-slot motor. For this reason a larger slot number may be beneficial in the 160mm motor, probably a 16-slot 18-pole or a 24-slot 16-pole design. The 16-slot 18-pole benefits from not requiring skew, the 24-slot 16-pole and 12-slot 8-pole designs needing to be skewed by half a slot pitch. The increased pole number would however lead to increased iron loss, although these are closer to the outside of the motor and would be easier to dissipate. These design possibilities will be investigated in the near future.

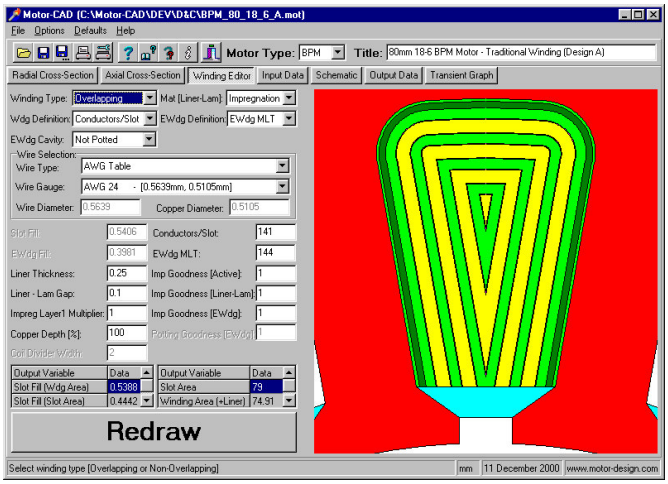


Fig. 7: Winding model showing copper/insulation layers in a traditional winding where are coils inserted into slots

Additional methods used to increase the winding dissipation include improved winding impregnation techniques and potting of the end-windings. Vacuum impregnation can eliminate air pockets within the winding. For instance the winding shown in Figs 6 & 7 benefit from a decrease in temperature rise of around 9% when the motors are perfectly impregnated compared to a 50% impregnated motor. The previous examples use a traditional impregnation material having a thermal conductivity of 0.2W/m/°C. However, new high temperature impregnation and potting materials are now available which have thermal conductivites of around 1W/m/°C. If one of the new materials were to be used in the two designs shown in Figs 6 & 7, a reduction in temperature rise of between 6% and 8% could be expected. If the end-windings were potted, a reduction in temperature rise of between 14% and 16% would be expected.

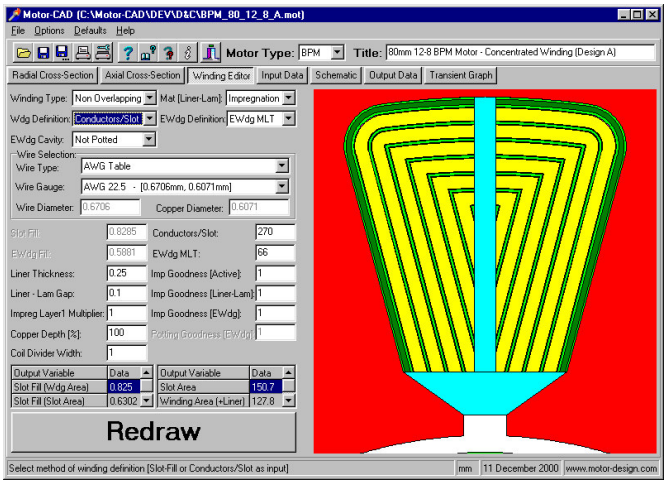


Fig. 8: Winding model showing the high slot-fills achievable in a precision wound non-overlapping winding

## Thermal Mathematical Models

Motor-CAD features efficient, accurate and robust mathematical algorithms for forced & natural convection, radiation and conduction. The particular convection model used for the various surfaces throughout the motor are automatically selected from a library of proven laminar and turbulent convection correlations [8-16]. Correlation formulations for open and closed channels and external surfaces of various shapes and orientations are included. Totally enclosed non-ventilated (TENV) and totally enclosed fan cooled (TEFC) forms of cooling are modelled. However, as the correlation formulations used are based upon dimensionless analysis of heat transfer they are also applicable to liquid cooling methods such as housing water jackets, shaft spiral grooves, wet rotor and wet stator cooling techniques. These are included in Motor-CAD. Rotation effects on convection cooling in the airgap are included within the model [15-16].

## Fin Design

The fin design is often given little attention in servo motors as they traditionally do not have a shaft mounted fan because they are intended to operate down to zero speed. The radial fin design shown in Fig 9 can however be used to increase the amount of natural convection from the housing [17]. In the case of the 80mm diameter motors presented earlier, a reduction in temperature rise of around 10% can be achieved

by adopting a radial fin design. There are special radial fin designs which allow similar dissipation when the motor is mounted vertically as when mounted horizontally [17].

External blower units are sometimes used to increase the output from servo motors [18]. If these are to be used, then one of the axial fin designs shown in Fig 10 would be beneficial.

Liquid Cooling

For applications requiring the ultimate in terms of torque/volume a liquid cooling arrangement similar to those shown in Fig 11 can be adopted. Natural convection typically has a heat transfer coefficient (W/m/°C) of between 5 & 25, forced convection of between 10 & 300 and liquid cooling of between 50 & 20000 [11].

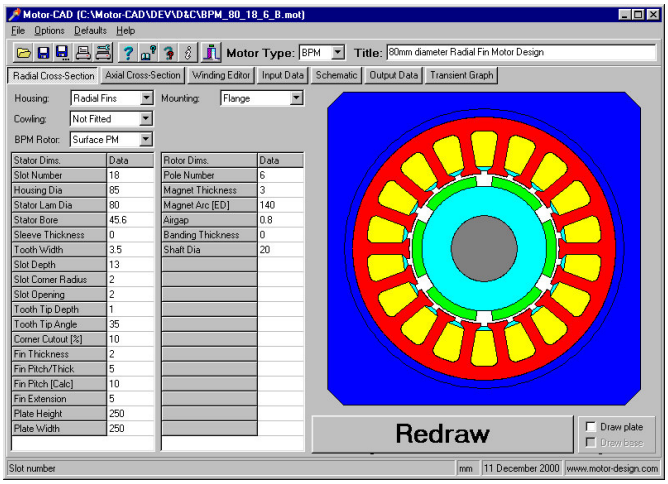


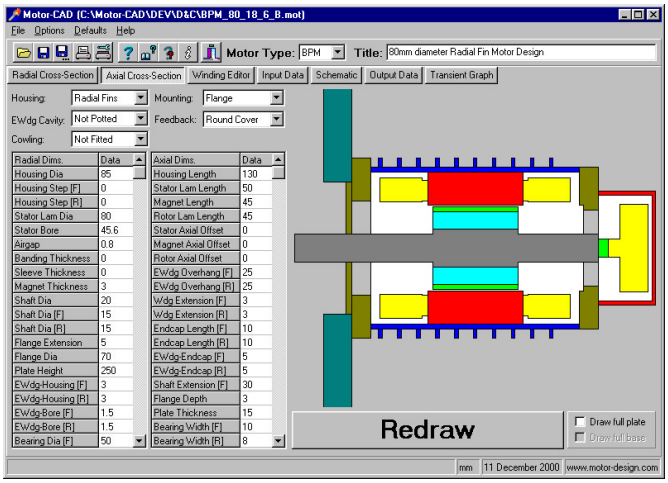


Fig 9: Motor with a radial fin design

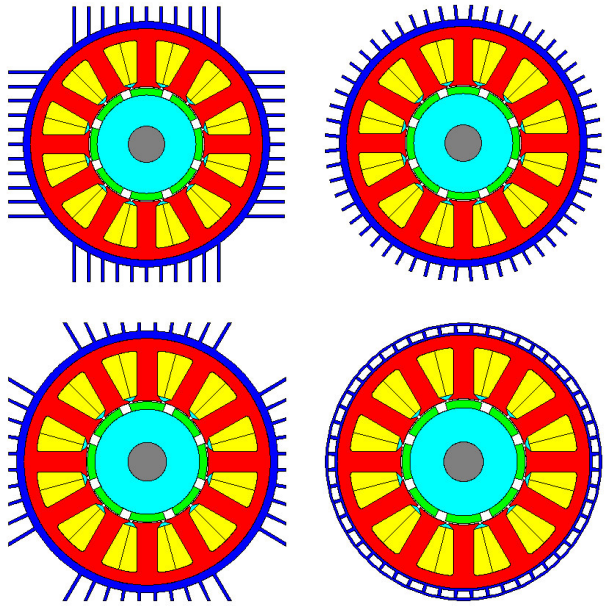

Fig 10 Examples of axial fin types

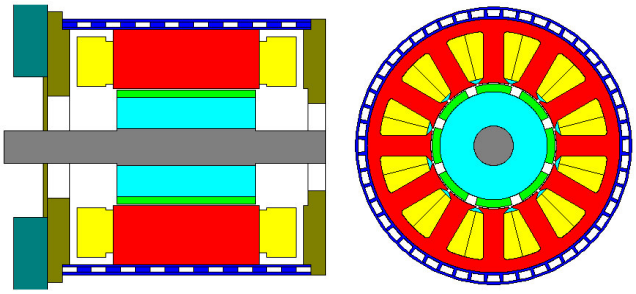

Fig 11 Examples of housing types suitable for liquid cooling

Mounting Arrangement

The mounting arrangement can have a significant impact on the thermal behaviour of the motor. In the servo motors shown in this paper, between 35 - 50% of the total loss is dissipated through the flange, the larger value being in the smaller motors. Such high figures are not uncommon as manufactures tend to use larger cooling plates than the standard plate sizes recommended by NEMA [19]. A motor must de-rate if it is unable to dissipate such powers into the device it is connected to.

Feedback Devices & Integrated Motors

When an encoder is used as a feedback device then this should be included in the model as they typically have temperature limits of between 80°C and 100°C. The encoder model used in Motor-CAD is shown in Figs 1 & 4. The encoder model can also be adapted to predict the temperature rise of control and power electronics attached to the rear of motors in integrated motor drives [20].

Magnet Temperature Limit

The magnet temperature is a key item to be calculated in permanent magnet motors, especially when Nd-Fe-B magnets are being used. This is because they are more sensitive to demagnetisation at elevated temperatures than Sm-Co. They also have a larger negative temperature coefficient of remanence which can lead to a significant reduction in torque/amp (Kt) at high temperatures. The trend is that the higher remanence Nd-Fe-B materials which are suited to high power densities also have a lower BH knee value so are more prone to demagnetisation. However new grades of Nd-Fe-B are emerging that have relatively high remanence (1.19T) and linear 3rd quadrant BH characteristics up to 180°C [21]. It is reassuring that the magnets are somewhat isolated from the main sources of loss (i.e. the stator copper and iron loss), so that under a severe overload condition, the magnet temperature rise is much slower than that of the stator components (Fig 13).

Transient Analysis

When carrying out transient analysis, thermal capacitances are connected to each of the nodes within the schematic shown in Fig 2. Each capacitance is calculated from the specific heat capacity and weight of the relevant motor components. The resulting set of partial differential equations are integrated to obtain the thermal transient characteristics.

Typical transient graphs are shown in Figs 11 & 12. Fig 11 shows the thermal transient produced when a motor is run at constant torque until the motor reaches its steady state temperature. It also shows the typical level of correspondence expected between measured and calculated transient characteristics when using an accurately defined model. It is also interesting to note that as with most motor rating tests, the motor current must be varied throughout the test to accommodate the torque constant (Kt) and iron losses which both reduce as the magnets heat up. These effects, in addition to the increase in winding resistance with temperature and the variation in losses with speed must all be taken account of within the program.

The transient graph shown in Fig 13 shows changes in temperature of the different motor components when driving a complex duty-cycle load. Duty-cycle analysis is essential in the majority of servo applications if the motor is to be driven to full potential without over-heating. This is illustrated in Figs 12 and 13 as the same motor is used for both calculations. When run continuously at rated torque the winding takes nearly 2 hours to reach its steady-state temperature. However when a severe duty cycle is used to load the machine, the same temperature is reached in around 15 seconds.

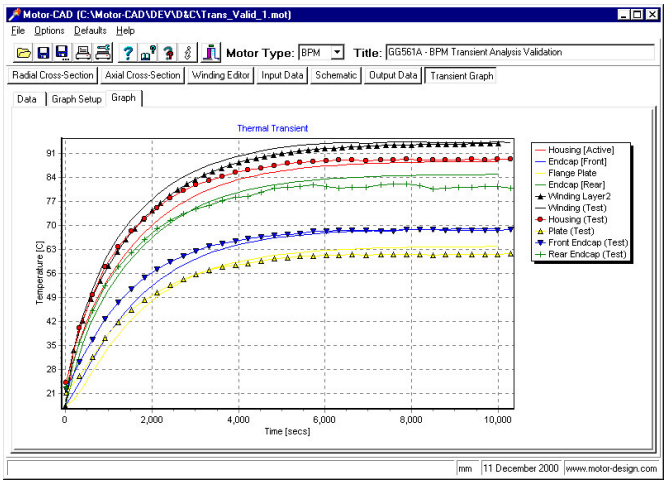


Fig. 12: Comparison of measured and calculated thermal transient for a small servo motor

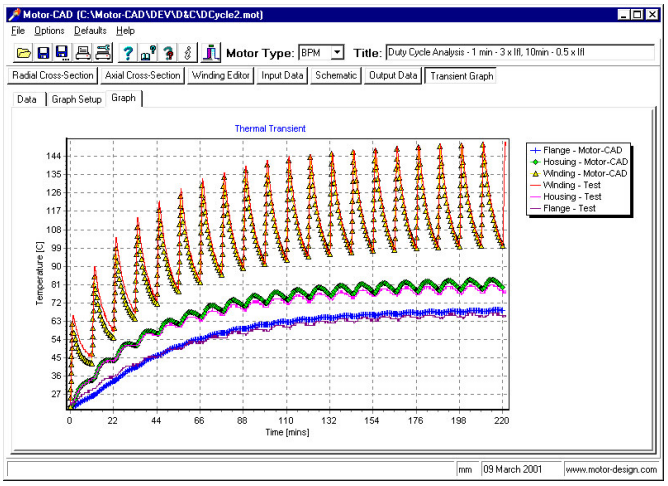


Fig. 13: Thermal transient for a small servo motor operating a duty cycle type load (test data also shown)

## Computational Fluid Dynamics (CFD)

Computational fluid dynamics (CFD) is a numerical tool that can be used to predict fluid flow and heat transfer in complex situations where standard solutions and experimental correlations are not available. It is particularly useful for modelling complex geometries and now gives the motor designer the opportunity to predict ventilation flows and heat transfer in areas such as end windings and salient pole rotors where little data is available. General purpose CFD codes have been available commercially for the past 10 years and now have the capability to be used in the design office. Whilst it is now possible to model a complete machine, this is generally beyond the resources of most companies in terms of computational capacity and manpower. CFD is much better suited to modelling parts of a machine and it gives the designer the opportunity to predict air flows and heat transfer coefficients for particular regions that can be used as input data for a lumped circuit analysis of the machine as a whole.

However, CFD modelling is not straight-forward and requires the user to have some knowledge of fluid flow and heat transfer. This is particularly true when modelling parts of a machine where it is important to define the correct boundary conditions in setting up the CFD model to ensure reliable results. An understanding of some of the limitations of CFD is also required particularly with regard to the fineness of the computational grid required to give accurate answers and in the choice of model for representing configurations involving rotation.

*Example – End windings of an Induction Motor*

An example is described here where CFD was used to predict heat transfer coefficients on the end windings of a high voltage TEFC induction motor. A fuller description of this work is presented in references [22-25]. The intention was to provide heat transfer coefficients that could then be used in a lumped-circuit analysis of the whole motor.

The geometry is complex as shown in Fig 14. Air flow is generated by the wafter blades mounted on the rotor and the air flows around the end windings and is recirculated back within the end region after transferring heat to the frame and end cover. Particular challenges for the CFD modelling are:

1) Modelling the rotation - The motion of the wafters and rotor bar extensions generate an inherently unsteady air flow due to interaction with the stationery end winding. This interaction between the rotor and the stator creates a complex flow pattern where the mean flow exhibits periodic fluctuations as the wafters and rotor bar extensions sweep past the end winding coils. This unsteady air flow has important influences on convective heat transfer.
2) The end winding has a complex open geometry with many small gaps in between the coils. This detail must be modelled accurately in order to provide detailed and accurate information on local heat transfer coefficients around the endwinding.

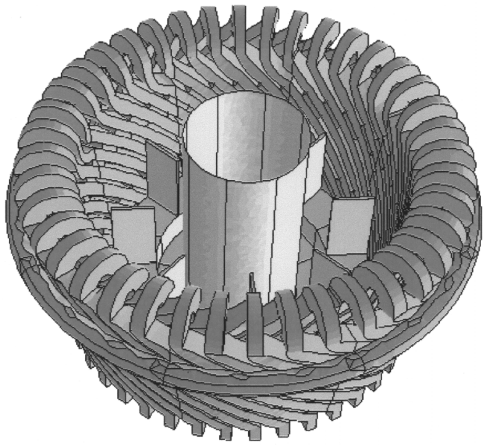

Fig. 14: End winding and rotor configuration (detail from CFD model (Fluent))

Modelling rotor-stator interaction

The best method of modelling rotor stator interaction is to use the *sliding mesh* technique. In this method, the rotor and stator are modelled using separate meshes. These slide relative to one another and a time dependent solution is obtained to represent the interaction in full.

However, at the time that this study was undertaken the CFD software used (Fluent) did not have the capability to use the sliding mesh technique and the *rotating reference frames* method was used instead, although this capability is now included in current versions of Fluent. In this method the rotor and stator are still modelled using two meshes. But it is assumed that there is steady flow at the interface between the rotor and stator and a time-averaged solution is adopted. This is much more economical in computing time but does not give a true representation of the unsteady nature of the rotor-stator interactions.

Modelling the geometry

It is only during the past few years or so that the widely used commercially available CFD codes have had the capability to model complex geometries with unstructured terahedral cells. Previously, regular hexahedral block type meshes had to be used with the constraint that rows of cells had to be continuous through the computational domain. This meant that complex geometries such as end windings could not practically be modelled. The use of Fluent, an

unstructured CFD code, greatly facilitated the modelling of the end winding geometry as shown in Fig 14.

CFD Model

The motor test rig had 8 wafter blades and, as a result of symmetry, only a 45 ° sector of the end region had to be modelled. This was done using the commercial CFD code Fluent. The 45° sector was modelled using about 500,000 cells and represented all of the main geometric features of the test motor. The rotor stator interaction was modelled using the rotating reference frames approach which assumes a steady flow at the interface between the rotor and stator. Several turbulence models were investigated including the k-ε model and the k-ε RNG model. It was found however, that the popular k-ε model performed the best, despite its acknowledged weakness in modelling highly swirling flows.

Experimental Measurements

To gain confidence in the use of CFD, experimental measurements were also made for comparison. The model of the end region of the test motor was constructed. The end windings from a real machine were used and mounted within a perspex cylinder to simulate the motor frame. The end of the rotor, end ring, wafters and the shaft were simulated and driven directly by a small motor mounted beneath the rig.

Air flow results

Fig 15 shows a typical result of a detailed comparison of the CFD predictions and measurements of air velocity magnitude on an axial traverse taken between the wafters and the end winding. This clearly shows that the overall air flow is well predicted over a range of rotational speed and that the velocity magnitudes in this strongly swirling flow are generally predicted to within 10% of the measurements.

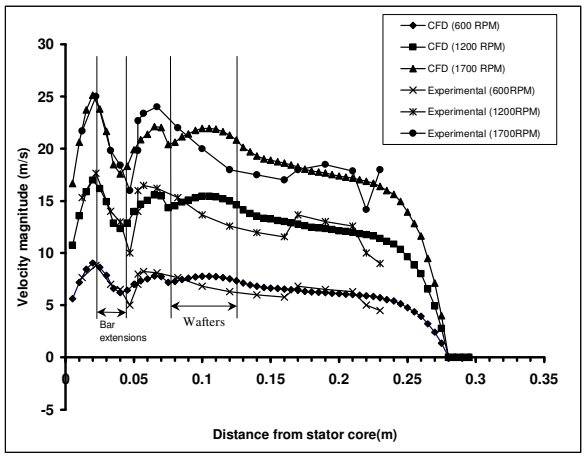


Fig. 15: Air velocity within the end region – (comparison of CFD and measurement)

Overall Heat Transfer Coefficients

Fig 16 shows a comparison of CFD predictions and measurements of overall heat transfer coefficients on the end winding coils and inside the motor frame in the end region. In each case the CFD predictions are lower than the measurements and are within 20%. The comparison is made over a speed range from 600 to 1700 rpm. The variation of heat transfer coefficient with speed is very well predicted and the predictions of the exponent for the variation of heat transfer coefficient with speed are almost identical to the measured values.

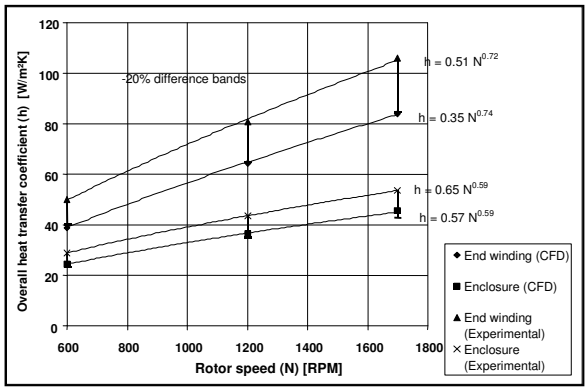


Fig. 16: Overall heat transfer coefficients on the end winding and inside frame (comparison of CFD and measurement)

Local End Winding Heat Transfer Coefficients

Fig 17 shows the variation of local heat transfer coefficient around an end winding coil. The location is on the inner face of the end winding opposite the wafter blades. In this position there is a strongly swirling flow on the inside surface of the end winding giving the highest heat transfer coefficient on the inside surface (position 4). Some air passes down the gaps between the coils and separates from the downstream side of the coil creating a region of recirculation. Consequently it is expected that the heat transfer coefficients would be higher on the side of the coil facing the swirl direction of the air flow (position 7) than on the downstream face (position 5). The region on the rear of the coil (position 6) has a low air flow and this has the lowest heat transfer coefficient The CFD predictions of heat transfer coefficient are all within 30% of the measured values and the variations with position are very well matched.

Fuller details of these results and also comparisons between CFD and experiment of the effect of various geometric variations are given in other publications [22-24]. Heat transfer coefficients on the frame of the motor were also modelled and found to be within 30% of experiment [24]. Comparisons of predicted windage loss were found to be within 20% of experimental measurement [24].

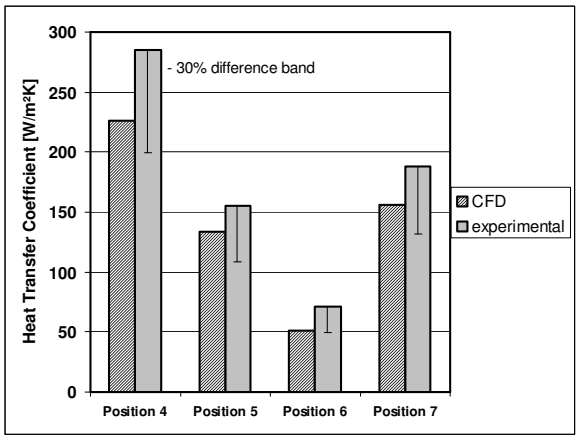


Fig. 17: Variation of heat transfer coefficient around an end winding coil (comparison of CFD and experiment)

Comments On CFD Predictions

In general the agreement of the CFD predictions with experiment is surprisingly good and getting results to within 20-30% is a big improvement on the previous situation where heat transfer coefficients were based on the best guess taken from experience. It would not be expected that measured heat transfer coefficients would agree exactly with the CFD predictions as there are a number of deficiencies in the modelling. Firstly, the end winding coils were assumed to be rectangular in cross section with sharp corners. In practice they have rounded corners and the surface is somewhat uneven due to the winding of the insulation around the coils. Rounded corners would in general give somewhat higher air flow rates and the uneveness in the surface means that it is difficult to position the heat flux gauges in truly representative positions. This, combined with manufacturing variations between coils, means that there would be expected to be variations in measured heat transfer coefficient between heat flux gauges mounted at the same position on different end winding coils.

However, perhaps the most important deficiency in the modelling is as a result of the use of the rotating reference frames method for modelling the rotation of the rotor. This assumes a steady flow at the interface between rotor and stator. In reality the flow is unsteady and the end winding coils would experience fluctuations in air flow as each wafter sweeps past a coil. This unsteadiness would increase the heat transfer coefficient and so it is only to be expected that the CFD predicted heat transfer coefficients are lower than the measured values.

Another factor is the CFD turbulence model. The k-epsilon model used in this study is known to be inaccurate in strongly swirling flows as it assumes that the turbulence is isotropic. The Reynolds Stress model is more appropriate for swirling flow but was not available in Fluent with rotating reference frames at the time this study was undertaken. However, it has the disadvantage of being more computationally intensive.

Potential for Design

The results of this study have shown that, even with known inadequacies in the CFD modelling, heat transfer coefficients within the end region of a TEFC induction motor on the end windings, frame and end shield can be predicted to within 30% accuracy. The predicted heat transfer coefficients are generally lower than those measured and so, for design purposes would give results that would be in error on the safe side; i.e. they would predict temperatures higher than would actually be achieved. CFD models of ventilation systems would thus yield heat transfer coefficients that could be used as boundary conditions to thermal models of complete machines. And these could be expected to give much more accurate results than has hitherto been possible.

A particular advantage of CFD is that much more detailed information can be obtained than would be available from experimental measurement, particularly in complex geometries such as end windings where access for measurement is very restricted. The detailed understanding of the flows and heat transfer that CFD can give should give insights to enable improvements in machine design to be made to enhance thermal performance. CFD techniques are rapidly becoming more cost effective in the development of new machines than more traditional methods of experimentation.

The CFD modelling carried out in this study was done on workstations that are typically used in industrial design offices today and the computation of one model typically took hours. Sliding mesh techniques are now commonly available and would be expected to give more accurate results. However, as they require solutions that are time dependent they will generally mean a substantial increase in computational effort required.

Application Of CFD In Design Office

In the early days of machine design, particularly where generators were concerned, many machines were slow speed and large in size. It was often the case that natural convection and the fanning effect of the rotor were sufficient to provide cooling. As machines have developed, higher ratings have been required from physically smaller packages. This concentration of losses in a smaller volume has only been possible by greatly improving the ventilation.

The mechanical power required to circulate the air around the cooling circuit is a significant loss in an air cooled machine and has a significant bearing upon the efficiency of such machines. The designer must therefore make every effort to minimise the windage loss and to maximise cooling

circuit effectiveness. With ever decreasing tolerances required on all design calculations and the high costs of getting it wrong, designers are venturing into areas where traditional predictive capabilities on their own are inadequate.

The standard design approach to air circuit modelling has taken the form of resistance network solutions for pressure drop and flow velocity. A major drawback with the network approach is that it is inherently one-dimensional, does not have any form of detailed air flow model (incorporating turbulence) and cannot therefore look at the localised cooling effects.

Modern CFD codes, such as Fluent, offer an alternative, attractive and efficient tool that can be used to explore optimal solutions for given design requirements. Sliding meshes and multiple frames of reference are just some of the advanced features of these packages which make them highly applicable to the rotating electrical machine product.

The high level of discretisation within a CFD solution gives detailed information on the localised air flow patterns. Whereas previously the arrows drawn upon a diagram of the air circuit could only indicate the intended path of the cooling air, it is now possible to address the movement of air with greater confidence.

Using the advanced graphical features of CFD codes, hot spots and the mechanisms that give rise to them can now be visualised. Thermal comparisons are an attractive means of validating CFD results as thermal tests are performed on most production jobs as a matter of course and increased detail can be obtained in the tests for minimal extra costs.

Time is at a premium on production work, with short lead times and high penalties for lateness. Beyond that which is required by the specification, there is very little scope to perform detailed air measurements on the majority of products shipped. Without this baseline of detailed test information, CFD as a design office tool is generally used for relative studies.

Some companies, such as ALSTOM Electrical Machines Ltd [25] have already started using CFD in the design of machines From simple wafters to more complex aerofoil section, fans are components that lend themselves to shape optimisation via CFD means. This is an area that has received considerable attention and with significant gains on some of the larger products. Indeed on certain products it has once again been possible to dispense with the use of fans altogether by harnessing the geometry of the machine to assist cooling.
Other areas to which CFD has been applied include:

- Cooler design, looking at the efficiency of the heat exchanger mechanism used to dissipate the heat from the cooling medium.
- Ventilation duct geometry, investigating the effect of change to the through paths within the core components of the machine.
- Envelope reduction, minimising the space requirement of the channels used to transfer air from the cooling surfaces to the heat exchanger.

As available hardware resource improves, it is now possible to consider a multidisciplinary approach to analysis. Within ALSTOM Electrical Machines Limited, CFD grids are transferred to Finite Element Analysis (FEA) packages on a regular basis, for additional thermal and structural analysis. Thermal constraints are also transferred with negligible user intervention. This provides a seamless airflow/thermal predictive capability.

**Conclusions**

This paper clearly demonstrates the advantages that can be gained from properly analysing the thermal characteristics of electric motors at the design stage. The Motor-CAD lumped circuit modelling package has been developed as a tool to assist the designer in this complex and important area of design. Some examples of how the package can aid the miniaturisation of permanent magnet motors have been shown, supported by data where appropriate.

Motors-CAD transient calculation capabilities have been demonstrated with test data. If a motor is to be driven to full potential without over-heating, the importance of carrying out transient duty-cycle analysis has also been shown.

CFD modelling now brings the ability to predict ventilation and heat transfer in areas of machines that have not been able to be addressed in the past. CFD has been found especially useful for predicting air flow and heat transfer coefficients for particular complex regions and the subsequent data then used to improve the simple models used in the lumped circuit analysis of the machine as a whole.

Companies are now investing in both lumped circuit and CFD techniques to enable them to optimise the designs of machines further in efforts to gain the competitive edge.

**References**


[1] Hendershot, J.R., Miller, T.J.E.: Design of Brushless Permanent-Magnet Motors, Magna Physics & Oxford Science Publications, 1994

[2] Hanselman, D.C.: Brushless Permanent-Magnet Motor Design, McGraw-Hill, 1994

[3] Hamdi, E.S.: Design of Small Elecrtical Machines, Wiley, 1994.

[4] SPEED information on the Cedrat web site – www.cedrat.com

[5] Staton, D.A.: Thermal Computer Aided Design – Advancing the Revolution in Compact Motors, IEEE International Electric Machines and Drives Conference (IEMDC), Boston, USA, 17-20 June 2001

[6] Staton, D.A., So E.: Determination of Optimal Thermal Parameters for Brushless Permanent Magnet Motor Design, IEEE-IAS Conference, St.Louis, Oct. 1998

[7] Staton, D.A.: Thermal Analysis of Naturally Ventilated Servo Motor Housings, 5th International Flotherm User Conference, Paris, 16-19 Sept. 1996.

[8] Ozisik, M.N.: Heat Transfer - A Basic Approach, McGraw Hill, 1995.

[9] Janna, W.S., Engineering Heat Transfer (S.I. Edition), Van Nostrand Reinhold (International), 1988

[10] Simonson, J.R.: Engineering Heat Transfer, Macmillan, 1988.

[11] White, F.M., Heat and Mass Transfer, Addison-Wesley.

[12] Bejan, A., Heat Transfer, John Wiley & Sons, Inc., 1993

[13] Incropera, F.P., DeWitt, D.P., Introduction to Heat Transfer, John Wiley & Sons, 1990

[14] Mellor, P.H., Roberts, D., Turner, D.R.: Lumped Parameter Thermal Model for Electrical Machines of TEFC Design. IEE Proc-B, Vol. 138, No. 5, Sept 1991.

[15] Taylor, G.I.: 'Distribution of Velocity and Temperature between Concentric Cylinders', Proc Roy Soc, 1935, 159, PtA, pp 546-578

[16] Gazley, C.: 'Heat Transfer Characteristics of rotating and axial flow bewteen concentric cylinders', Trans ASME, Jan 1958, pp.79-89.

[17] Unimotor knocks the competition out cold, Torqueback magazine, Control Techniques Dynamics Ltd, Vol 1, Issue 3.

[18] Fan cowlings boost torque by up to 87%, Drives & Controls, Oct. 1999.

[19] Nema Standards:, Publication No. MG7, Revision Jan. 26, 1993.

[20] Technology Update, Drives & Controls, May 2000

[21] Sumitomo Numax Catalogue, 1999

[22] Mugglestone J., Lampard D. and Pickering S.J., 'Effects of end winding porosity upon the flow field and ventilation losses in the end region of TEFC induction machines', IEE Proc.- Electr. Power Appl., Vol. 145, No. 5 pp423-428, September 1998.

[23] Mugglestone J, Pickering S.J. & Lampard D, 'Prediction of heat transfer from the end winding of a TEFC strip-wound induction motor'. Proc of IEMDC'99, IEEE Intl, Electric Machines and Drives Conf, Seattle, USA, May 1999, pp 484-486.

[24] Mugglestone J, Pickering S.J. and Lampard D, 'Effect of Geometry Changes on the Flow and Heat Transfer in the End Region of a TEFC Induction Motor'. Proc of 9th IEE Intl. Conf. On Electrical Machines and Drives, Canterbury, UK, Sept 99, pp40-44.

[25] Pickering, SJ, Lampard, D, Mugglestone, J, Shanel, M and Birse, D "Using CFD in the Design of Electrical Motors and Generators", Chapter 12 in *Computational Fluid Dynamics in Practice.* Ed. by Norman Rhodes, Published by Professional Engineering Publishing, 2001, ISBN 1 86058 352 0.